Neurocomputing 000 (2017) 1–7

Contents lists available at ScienceDirect

Neurocomputing

journal homepage: www.elsevier.com/locate/neucom

Application of self-organizing map to failure modes and effects analysis methodology

Wui Lee Chang, Lie Meng Pang, Kai Meng Tay*

Faculty of Engineering, Universiti Malaysia Sarawak, Sarawak, Malaysia

ARTICLE INFO

Article history:
Received 23 September 2015
Revised 3 December 2015
Accepted 10 April 2016
Available online xxx

Keywords:
Failure modes and effects analysis
Clustering
Visualization
Self-organizing map
Risk Priority Number Interval

ABSTRACT

In this paper, a self-organizing map (SOM) neural network is used to visualize corrective actions of failure modes and effects analysis (FMEA). SOM is a popular unsupervised neural network model that aims to produce a low-dimensional map (typically a two-dimensional map) for visualizing high-dimensional data. With regards to FMEA, it is a popular methodology to identify potential failure modes for a product or a process, to assess the risk associated with those failure modes, also, to identify and carry out corrective actions to address the most serious concerns. Despite the popularity of FMEA in a wide range of industries, two well-known shortcomings are the complexity of the FMEA worksheet and its intricacy of use. To the best of our knowledge, the use of computation techniques for solving the aforementioned shortcomings is limited. The use of SOM in FMEA is new. In this paper, corrective actions in FMEA are described in their severity, occurrence and detect scores. SOM is then used as a visualization aid for FMEA users to see the relationship among corrective actions via a map. Color information from the SOM map is then included to the FMEA worksheet for better visualization. In addition, a Risk Priority Number Interval is used to allow corrective actions to be evaluated and ordered in groups. Such approach provides a quick and easily understandable framework to elucidate important information from a complex FMEA worksheet; therefore facilitating the decision-making tasks by FMEA users. The significance of this study is two-fold, viz., the use of SOM as an effective neural network learning paradigm to facilitate FMEA implementations, and the use of a computational visualization approach to tackle the two well-known shortcomings of FMEA.

© 2017 Elsevier B.V. All rights reserved.

1. Introduction

Failure modes and effects analysis (FMEA) is an effective problem prevention and risk analysis methodology for defining, identifying, and eliminating failures of a system, design, process, or service [1]. A search in the literature reveals that FMEA was extensively used in a wide range of application domains, e.g., aerospace [2], automotive [1], nuclear [3], electronic [4], manufacturing [5,6], chemical [7], mechanical [8], healthcare and hospital [9], and agriculture [10]. FMEA usually starts with identifying the failure modes of a system or process, understanding the causes and effects of each failure mode, and determining suitable corrective actions to eliminate or reduce the risk of the respective failure modes [1]. Traditionally, the risk of a failure mode is determined by a Risk Priority Number (RPN) model [1]. The RPN model considers three risk factors as its inputs, i.e. severity (S), occurrence (O), and detection (D), and produces an *RPN* score (i.e. multiplication of S, O, and D) as the output [1]. S and O are seriousness and frequency of a failure mode and its root cause(s), respectively, while D is the effectiveness of the existing measures in detecting a failure mode before the effect of the failure mode reaches the customer(s) [1].

While the effectiveness of FMEA has been demonstrated, three shortcomings pertaining to practical implementation of FMEA are as follows. (1) its risk evaluation and prioritization issues [2,5,11,12]; (2) the complexity of the FMEA worksheet [13]; and (3) its intricacy of use [13,14]. The first shortcoming is well known and much research works have been conducted [2,11]. The first shortcoming suggests that the traditional RPN model is susceptible to a number of limitations, among the popular are, (1) relative importance among S, O and D is not taken into consideration [2], (2) different combinations of S, O and D may produce exactly the same value of RPN, but their hidden risk implications may be totally different [5], (3) the three risk factors are difficult to be precisely evaluated [11], (4) the mathematical formula for calculating RPN is questionable [11] and etc. Besides, according to a review from [11], the existing risk evaluation methods can be grouped into five categories, i.e., multi-criteria decision making methods, mathematical programming methods, artificial intelligence methods, integrated methods, and other methods.

* Corresponding author.
E-mail addresses: kmtay@unimas.my, tkaimeng@yahoo.com (K.M. Tay).

http://dx.doi.org/10.1016/j.neucom.2016.04.073
0925-2312/© 2017 Elsevier B.V. All rights reserved.

Please cite this article as: W.L. Chang et al., Application of self-organizing map to failure modes and effects analysis methodology, Neurocomputing (2017), http://dx.doi.org/10.1016/j.neucom.2016.04.073

Even though much works on the first shortcoming has been reported, to the best of our knowledge, little effort was on the other two shortcomings. The second shortcoming suggests that FMEA worksheet is complex [13]. Entries in a FMEA worksheet are voluminous [13]. An example of an FMEA table (e.g. see [1], pages 231–242) could take up to 11 pages. The third shortcoming suggests that the FMEA worksheet is hard to produce [13,14], hard to understand and read, as well as hard to maintain [13,14]. It was reported that FMEA, as implemented in Microsoft Excel, is unwieldy with much mouse scrolling required [13]. Too much mouse scrolling detracts FMEA users' mental representation of the FMEA worksheet as a whole, and prevents FMEA users from seeing the overall structure of the FMEA worksheet [13]. Failure analysis matrix (FAM) worksheet, a much smaller worksheet that requires less mouse scrolling, was then proposed as a finder and gentler alternative to, but not as a total replacement for, FMEA worksheet [13]. Other efforts to computerize or automate design FMEA were also reported [14-16]. However, it is not clear how these works [14-16] could be applied to process FMEA, or FMEA in general.

The main aim of this paper is to examine the use of the self-organizing map (SOM) neural network for analyzing (i.e., both clustering and visualization) failure modes and corrective actions in FMEA. The focus of this paper is on clustering and visualization of corrective actions. Fuzzy adaptive resonance theory (ART) was firstly used by Keskin and Özkan [17] to tackle the problem whereby different combinations of S, O, and D could produce the same *RPN* scores. In addition to this reason, we further justified the advantages of using clustering and visualization methods in FMEA, as follows: (1) clustering and visualization deals with the original S, O, and D scores directly [18]; (2) clustering and visualization allows the failure modes to be compared and visualized in the input space as groups of information [18]; (3) the use of the original S, O, and D scores (instead of the mapped S, O, and D scores into a common domain) avoids loss of information or modification of important information for decision making purposes [18].

In our previous work [19], clustering and visualization methods were suggested as a solution for tackling the two above-mentioned shortcomings related to FMEA implementation, i.e., the complexity of the FMEA worksheet and its intricacy of use. From our literature research, limited investigations on using computing techniques to solve the aforementioned issues have been reported so far. Visualization serves as a communication means between FMEA worksheet and its users [19]. A good visualization (or effective communication) is important because (1) it presents the corrective actions as a structure that is easy to understand, as compared with the original corrective actions in complex FMEA worksheets [19]; (2) it allows users to access or analyze FMEA with a large number of corrective actions quickly, which may not be otherwise possible [19]; (3) it provides users an overview of all corrective actions, which mitigates the problem in having a good understanding and insight into the overall FMEA exercise in situations where no visualization is available [19]; and (4) it leads to more efficient processes for making decisions and taking actions [19].

In our previous work, two incremental-learning neural network models (i.e., fuzzy ART [20] and evolving tree [21]) were used for analysis of failure modes in FMEA. In [18], fuzzy ART was used to cluster failure modes to groups based on their similarity, in which failure modes within a cluster share higher similarity measures, as compared to those associated with other clusters. In [19], evolving tree was used for analyzing (i.e., both clustering and visualization) failure modes in a complicated FMEA worksheet, instead of just performing clustering only as in the use of fuzzy ART [18]. Failure modes were transformed to a tree structure for better visualization [19]. Such visualization is useful as it provides a quick and easily understandable representation of the FMEA worksheet, which is usually complex and lengthy, to facilitate decision making tasks. Two concepts, i.e., risk interval and risk ordering of clusters, were introduced to allow failure modes or corrective actions to be analyzed in a group [18,19].

Instead of fuzzy ART and evolving tree, SOM is used for both clustering and visualization of corrective actions in FMEA, in this paper. To the best of our knowledge, the use of SOM in FMEA is new. SOM is a neural network capable of mapping high dimensional data samples onto a lower dimensional space and representing them as nodes [22-24]. It also provides a topological view of the underlying data structure [22-24]. In this paper, SOM is used as a visualization aid for FMEA users to see the relationship among corrective actions via a color map. Color information from the SOM map is then included to the FMEA worksheet for better visualization. SOM is chosen because of its topological preserving feature [23]. However, a drawback of using SOM is that map size has to be predefined and this may lead to experiments with different sized maps, trying to obtain the optimal result [21]. In addition, the proposed risk interval and risk ordering equations for different groups of failure modes from [18] are used to allow corrective actions to be ordered and evaluated in groups. To evaluate the proposed method, benchmark information from [1] (pages 231–242) is used. The experimental results show that the complicated and lengthy FMEA worksheets can be clustered and visualized as a comprehensible SOM map with color. Inclusion of color information from the SOM map to the FMEA worksheet could provide FMEA users a good understanding and insight of corrective actions.

This paper is organized as follows. In Section 2, the background of FMEA and the RPN model is explained. In Section 3, the use of SOM in FMEA is described. In Section 4, the experimental results are presented and discussed. Finally, concluding remarks are provided in Section 5.

2. Preliminaries

To make this paper self-contained, the RPN model is explained and discussed.

2.1. Severity, occurrence, detection and Risk Priority Number

Traditionally, FMEA adopts an RPN model, which considers three risk factors, i.e., S, O, and D, for prioritizing the corrective actions. These three risk factors are defined as follows.

Definition 1. A risk factor, $X \in [S, O, D]$, is considered. Variables s, o, and d are the elements of S, O, and D, respectively, i.e., $s \in$ S, $o \in$ O, and $d \in D$. The lower and upper boundaries of S are represented by $\underline{s}$ and $\bar{s}$, respectively. Similarly, the lower and upper boundaries of O and D are represented by $\underline{o}$ and $\bar{o}$, as well as $\underline{d}$ and $\bar{d}$, respectively. In this paper, an $S \times O \times D$ bounded space, which is a combination of S, O, and D risk factors, is further considered.

An RPN model produces an *RPN* score. The space containing all *RPN* scores is defined as follows.

Definition 2. The *RPN* space is the output space containing all possible *RPN* scores. The lower and upper boundaries of the RPN space are represented by $\underline{RPN}$ and $\overline{RPN}$, respectively. Ideally, the *RPN* space follows a monotonic, ordered sequence, i.e., the higher the *RPN* score, the higher the risk.

The aim of the traditional FMEA is to prioritize corrective actions. A corrective action in FMEA is described in their S, O and D scores, i.e., [s, o, d]. A set of corrective actions as defined in Definition 3 is considered.

Definition 3. m corrective actions, described as $\overline{x_k} = [s_k \in \text{S}, o_k \in \text{O}, d_k \in \text{D}]$, $k = 1, 2, 3, \ldots, m$, is considered.

Please cite this article as: W.L. Chang et al., Application of self-organizing map to failure modes and effects analysis methodology, Neurocomputing (2017), http://dx.doi.org/10.1016/j.neucom.2016.04.073

Traditionally, the *RPN* score for a corrective action, described as $\overline{x_k} = [s_k, o_k, d_k]$, is obtained using Eq. (1). Eq. (1) can be viewed as a mapping of [*s, o, d*] to the *RPN* space.

$$RPN_k = s_k \times o_k \times d_k. \quad (1)$$

3. The proposed approach

In this section, the SOM model for FMEA application is described in details, as follows. The idea of RPN Interval is further explained.

3.1. The SOM-based approach

A two-dimensional topological map with $x \times y$ neurons is considered. Each neuron is denoted as N_l, where $l = 1, 2, 3, \ldots, n = x \times y$, and associated a weight vector, i.e., $W_l = [w_{l,S}, w_{l,O}, w_{l,D}]$. The important steps of SOM are as follows.

Step 1: Initializing a two-dimensional topological map (i.e., a $x \times y$ map) with n neurons. x and y need to be predefined. The weight vector associated to each neuron, W_l is initialized randomly.
Step 2: Fetching corrective actions, $\overline{x_k}$, where $k \in \{1: m\}$ (See Definition 3).
Step 3: Setting $k = 1$.
Step 4: Spell out the best matching unit (BMU) for $\overline{x_k}$.
4.1. Using an Euclidean distance measure (Eq. (2)) to find the similarity between $\overline{x_k}$ and N_l, where $l = 1, 2, 3 \ldots, n$.

$$\text{Euclidean distance measure } (N_l, \overline{x_k}) = \sqrt[2]{\left(w_{l,S} - s_k\right)^2 + \left(w_{l,O} - o_k\right)^2 + \left(w_{l,D} - d_k\right)^2} \quad (2)$$

4.2. Tracking the neuron with the smallest Euclidean distance measure, i.e., the BMU and denoted it as N_{BMU}. Weight vector associated to N_{BMU} is denoted as $W_{BMU} = [w_{BMU,S}, w_{BMU,O}, w_{BMU,D}]$
Step 5: Updating W_l. W_l is updated using the Kohonen learning rule, described in Eq. (3).

$$W_l(t+1) = W_l(t) + h_{BMU,l}(t)[\overline{x_k} - W_l(t)]. \quad (3)$$

$t = 0, 1, 2, \ldots$ is a step index. $h_{BMU,\,l}(t)$ is the neighbourhood function, as defined in Eq. (4).

$$h_{BMU,l}(t) = \alpha(t) exp\left(-\frac{\sqrt[2]{\left(w_{BMU,S} - w_{l,S}\right)^2 + \left(w_{BMU,O} - w_{l,O}\right)^2 + \left(w_{BMU,D} - w_{l,D}\right)^2}}{2\sigma^2}\right) \quad (4)$$

where, $\alpha(t)$ is the learning rate, and σ is the distance between N_l and N_{BMU} on the topological map. $\alpha(t)$ is a monotonically decreasing function of t. In this paper, $\alpha(t)$ is determined with Eq. (5).

$$\alpha(t) = 1 - t/100 \quad (5)$$

Step 6: Setting $k = k + 1$.
Step 7: If $k = m$, go to Step 8. Else, go to Step 4.
Step 8: If $W_l(t+1) - W_l(t) \le 0.00001$, in which $W_l(t+1) - W_l(t) = max\ (W_{l,S}(t+1) - W_{l,S}(t),\ W_{l,O}(t+1) - W_{l,O}(t), W_{l,D}(t+1) - W_{l,D}(t))$, go to Step 9. Else, go to Step 3.
Step 9: End.
Steps 1 to 9 generate a two-dimensional topological map, with $x \times y$ neurons. Each neuron represents a cluster, and W_l is the centroid of the cluster in the $S \times O \times D$ space. The topological map also describes the position of each cluster in a two-dimensional space. A corrective action, described as $\overline{x_k} = [s_k, o_k, d_k]$, belongs to the cluster with smallest $(W_{l,S} - s_k)^2 + (W_{l,O} - o_k)^2 + (W_{l,D} - d_k)^2$.

3.2. RPN Interval of a cluster

In this paper, the RPN scores associated with the corrective actions in each cluster is represented as an RPN Interval, i.e., $RPN_l = [\underline{RPN_l}, \overline{RPN_l}]$. Eq. (1) is used to obtain the *RPN* score of each $\overline{x_k}$ pertaining to a cluster (i.e., $k \in N_l$), and is denoted as RPN_k. The RPN Interval of N_l that contains a group of corrective actions is obtained using Eqs. (6) and (7).

$$\underline{RPN_l} = \min\ (RPN_k,\ \text{where } k \in N_l) \quad (6)$$

$$\overline{RPN_l} = \max\ (RPN_k,\ \text{where } k \in N_l) \quad (7)$$

4. Experimental results and discussion

4.1. Benchmark information

In this section, experiments are conducted with benchmark information from [1] (pages 231–242), a 11-page FMEA worksheet. It is a design FMEA for an industrial grade APC connector. A part of the FMEA worksheet is depicted in Fig. 1. Column "Product requirement" is the function of the sub-components. Column "Potential failure mode" is the list of potential failure modes for the sub-components. Column "Potential effects of failure" lists potential consequences if a potential failure mode occurs. Potential root causes of a failure mode are listed in column "Potential cause of failure". Corrective actions are listed in column "Current control, $\overline{x_k}$". Each corrective action is labeled as k, and indicated in column "k". S, O and D scores for $\overline{x_k}$ are listed in columns "s_k", "o_k" and "d_k", respectively. RPN for $\overline{x_k}$ is obtained using Eq. (1) and listed in column "RPN_k" .

For example, one of the product requirements is "Seal at the enclosure" and it is associated with a potential failure mode, namely "Leakage at enclosure". There are four potential effects for "Leakage at enclosure", i.e., "Equipment failure (Physical)", "Fire", "Equipment failure (electric)" and "Rework/Maintenance". One of the potential causes for "Leakage at enclosure" is ""O" Ring". Current control for the root cause is "Visual", and is labeled as $\overline{x_1}$, in which $k = 1$. The S, O and D scores for $\overline{x_1}$ are 8, 2, and 5, respectively. The RPN for $\overline{x_1}$ is obtained via Eq. (1). $RPN_1 = 8 \times 2 \times x5 = 80$ is obtained. S, O and D scores for $\overline{x_{55}}$ is missing. In this paper, $s_{55} = 0$, "$o_{55} = 0$", and "$d_{55} = 0$", is assumed.

The complete benchmark FMEA worksheet is voluminous and lengthy. It is not easy to comprehend and maintain the FMEA worksheet. There are 77 corrective actions, i.e., $m = 77$. Thus, the proposed SOM-based approach from Section 3 is used to cluster and visualize the 77 corrective actions.

4.2. Simulation results and discussions

4.2.1. Clustering and visualization of corrective actions

In this paper, procedure in Section 3.1 is used to cluster and visualize corrective actions. A number of x and y settings are experimented. The best map obtained with settings $x = 2$ and $y = 3$. Fig. 2 depicts the 2×3 SOM map with six neurons generated. These neurons are labeled as N_1, N_2, N_3, N_4, N_5 and N_6. Each neuron represents a group of corrective actions. There are 2, 13, 15, 24, 5 and 18 corrective actions, for N_1, N_2, N_3, N_4, N_5 and N_6, respectively.

These six groups of corrective actions can also be depicted in the S × O × D space, as shown in Fig. 3. Details for the simulation outcome are also tabulated in Table 1. The first group, represented as N_1 (i.e., $l = 1$), is associated with weight vectors of 2.0, 9.0 and 1.0 ($w_{1,S}$, $w_{1,O}$ and $w_{1,D}$, respectively). The center of the first group is represented by the weight vectors of N_1 (i.e., 2.0, 9.0 and 1.0) and shown in Fig. 3. There are two corrective actions associated

Please cite this article as: W.L. Chang et al., Application of self-organizing map to failure modes and effects analysis methodology, Neurocomputing (2017), http://dx.doi.org/10.1016/j.neucom.2016.04.073

Product requirement	Potential failure mode	Potential effects of failure	Potential cause of failure	Existing conditions						Recommended actions and status
				Current controls, $\overline{x_k}$	k	s_k	o_k	d_k	RPN_k	
Seal at the enclosure	Leakage at enclosure	1. Equipment failure (physical)	**"O" Ring**	Visual	1	8	2	5	80	Review design of "O" ring for color and fit
		2. Fire	…Size	Cert.	2	6	1	9	54	
			…Cracked	Visual	3	3	1	9	27	
		3. Equipment failure (electric)	…Out of groove	Visual	4	6	2	3	36	
			Body …Cracked hub	Visual	5	2	1	10	20	
		4. Rework/maintenance	…Undersize hub	Gauge	6	4	1	9	36	
			Flash on stopping shld	Visual	7	4	1	9	36	
Seal at the conduit	Leakage at conduit	1. Equipment failure(physical)	**Conduit** Size	Industry standard	8	6	5	8	240	Look for new vendor
		2. Fire	Burrs	Stuffer	9	3	2	9	54	
		3. Equipment failure (electric)	**Body** Scratched	Visual	10	3	1	9	27	
			Cracked	Visual	11	3	1	9	27	
		4. Rework/maintenance	Dimensional	Control Chart	12	4	1	9	36	
			Installation Partial insertion	Stuffer	13	3	4	9	108	Review design to allow wider range of cond. I.D.
Strain relief	Strain relief and pullout resistance	1. Loss of conductor protection	**Part Cracked** …Over torque	Stuffer	14	8	1	1	8	
		2. Equipment failure (electrical)	…Vibration	None	15	8	1	2	16	
			…Abuse	None	16	8	2	1	16	
		3. Rework/maintenance	**Dimensional** …Gland/body thread	Control chart	17	8	1	2	16	
		4. Equipment damage (mechanical)	…Unfilled parts	Visual	18	8	1	1	8	
		5. Fire	**Installation** …Not tight	Stuffer	19	8	3	2	48	
			…Contaminant	Stuffer	20	8	2	2	32	Review installation instructions

Fig 1. A part of FMEA worksheet from [1] (see pages 231–242).

Table 1
Corrective actions analysis with the 2 × 3 SOM map.

Neuron, N_l	$w_{l,S}$	$w_{l,O}$	$w_{l,D}$	RPN_l	$\overline{RPN_l}$	List of corrective actions
1	2.0	9.0	1.0	9	27	$\overline{x_{21}}$, and $\overline{x_{56}}$
2	3.2	1.5	1.5	3	20	$\overline{x_{22}}$, $\overline{x_{32}}$, $\overline{x_{55}}$, $\overline{x_{57}}$, $\overline{x_{58}}$, $\overline{x_{59}}$, $\overline{x_{60}}$, $\overline{x_{61}}$, $\overline{x_{62}}$, $\overline{x_{63}}$, $\overline{x_{71}}$, $\overline{x_{72}}$, and $\overline{x_{77}}$. $\overline{x_{55}}$ is ignored.
3	7.9	1.4	8.8	54	168	$\overline{x_2}$, $\overline{x_{23}}$, $\overline{x_{24}}$, $\overline{x_{25}}$, $\overline{x_{33}}$, $\overline{x_{37}}$, $\overline{x_{40}}$, $\overline{x_{41}}$, $\overline{x_{42}}$, $\overline{x_{43}}$, $\overline{x_{68}}$, $\overline{x_{69}}$, $\overline{x_{73}}$, $\overline{x_{74}}$, and $\overline{x_{75}}$
4	7.8	1.2	1.3	6	48	$\overline{x_{14}}$, $\overline{x_{15}}$, $\overline{x_{16}}$, $\overline{x_{17}}$, $\overline{x_{18}}$, $\overline{x_{19}}$, $\overline{x_{20}}$, $\overline{x_{26}}$, $\overline{x_{27}}$, $\overline{x_{44}}$, $\overline{x_{45}}$, $\overline{x_{46}}$, $\overline{x_{47}}$, $\overline{x_{48}}$, $\overline{x_{49}}$, $\overline{x_{50}}$, $\overline{x_{51}}$, $\overline{x_{52}}$, $\overline{x_{53}}$, $\overline{x_{54}}$, $\overline{x_{64}}$, $\overline{x_{65}}$, $\overline{x_{66}}$, and $\overline{x_{67}}$
5	7.6	1.4	4.0	32	80	$\overline{x_1}$, $\overline{x_4}$, $\overline{x_{28}}$, $\overline{x_{29}}$, and $\overline{x_{30}}$
6	3.8	2.5	9.0	20	270	$\overline{x_3}$, $\overline{x_5}$, $\overline{x_6}$, $\overline{x_7}$, $\overline{x_8}$, $\overline{x_9}$, $\overline{x_{10}}$, $\overline{x_{11}}$, $\overline{x_{12}}$, $\overline{x_{13}}$, $\overline{x_{31}}$, $\overline{x_{34}}$, $\overline{x_{35}}$, $\overline{x_{36}}$, $\overline{x_{38}}$, $\overline{x_{39}}$, $\overline{x_{70}}$, and $\overline{x_{76}}$

Please cite this article as: W.L. Chang et al., Application of self-organizing map to failure modes and effects analysis methodology, Neurocomputing (2017), http://dx.doi.org/10.1016/j.neucom.2016.04.073

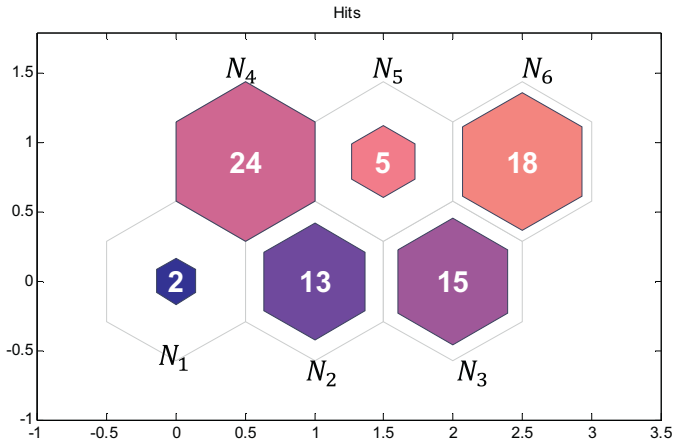


Fig 2. Corrective actions in the 2 × 3 SOM map.

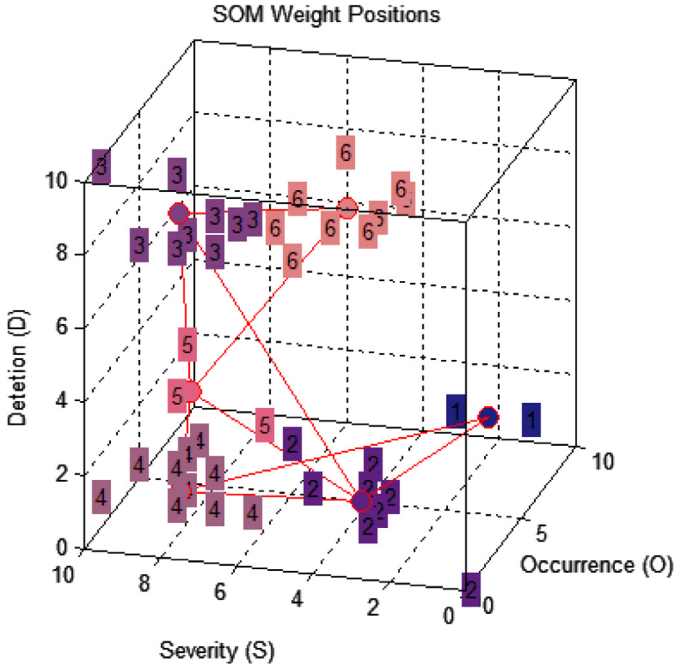


Fig 3. Corrective actions in the S × O × D space.

to the first group, i.e., $\overline{x_{21}}$, and $\overline{x_{56}}$. The RPN Interval for the first group is 9 to 27, using Eqs. (1), (6) and (7). In short, the first group of corrective actions is that with high O score, but low S and D scores. In the second group, there are 13 corrective actions, listed in Table 1. The weight vectors or center for the second group are 3.2, 1.5 and 1.5, and depicted in the S × O × D space in Fig. 3. $\overline{x_{55}}$ is ignored, as its S, O and D scores is missing. Thus, RPN Interval for the second group is 3 to 20.

The third group, i.e., N_3, is a relatively large group with 15 corrective actions. It is associated to weight vectors of 7.9, 1.4 and 8.8. Again, it is depicted in the S × O × D space in Fig. 3. The RPN Interval for the third group is 54 to 168. In this paper, each group of corrective actions is represented by a color. For example, the third group is represented by purple. A member of the third group, i.e., $\overline{x_2}$, is labeled as purple in the FMEA worksheet (see Fig. 1). In this paper, we suggest to include the color information from Figs. 2 and 3 to Fig. 1 for better visualization. In Fig. 1, corrective actions belong to the fourth group (i.e., $\overline{x_{14}}$, $\overline{x_{15}}$, $\overline{x_{16}}$, $\overline{x_{17}}$, $\overline{x_{18}}$, $\overline{x_{19}}$, and $\overline{x_{20}}$) are colored as red-violet. The corrective actions belong to the fifth group (i.e., $\overline{x_1}$ and $\overline{x_4}$) are then colored as pale red-violet in Fig. 1.

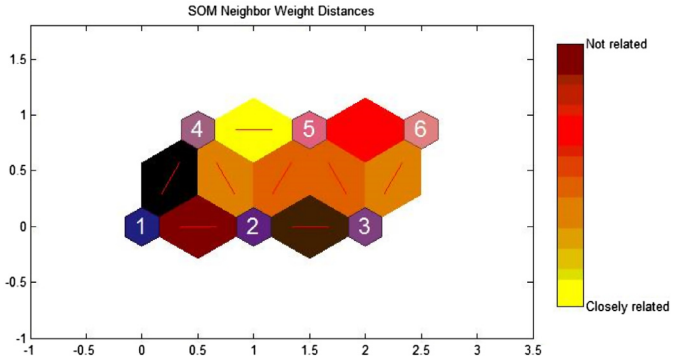


Fig 4. Relationships among groups of corrective actions in the topological neighborhood map.

The corrective actions belong to the sixth group, i.e., $\overline{x_3}$, $\overline{x_5}$, $\overline{x_6}$, $\overline{x_7}$, $\overline{x_8}$, $\overline{x_9}$, $\overline{x_{10}}$, $\overline{x_{11}}$, $\overline{x_{12}}$, and $\overline{x_{13}}$ are colored as pink, in Fig. 1.

4.2.2. Ordering of corrective actions in groups and decision making

It is important to order corrective actions for decision making. Ordering of 77 corrective actions is possible, but may not be so easy to be comprehended by the FMEA users. Using the proposed SOM-based approach, corrective actions are clustered to groups and ordered in groups. From Table 1, $N_2 < N_1/N_4 < ([N_5 < N_3]/N_6)$ can be concluded. In this paper, "/" is used to represent the subsethood of clusters, considering their RPN Interval (i.e., $[\underline{RPN_l}, \overline{RPN_l}]$). The RPN Interval for N_1(i.e., [9, 27]) is a subset of N_4 (i.e., [6, 48]) and they are not ordered. Both N_4 and N_1 are greater than N_2. The RPN Interval for N_2, N_4 and N_1 is lower than that of N_3, N_5, and N_6. The RPN Interval for N_5 is lower than that of N_3. The RPN Interval for N_3 and N_5 are a subset of N_6.

Such relatively simple ordering outcome provides FMEA users a simpler view of the 77 corrective actions. Besides that, some FMEA users may want to focus on corrective actions with high S scores or high O scores. From Table 1, corrective actions with high O scores are associated to N_1. Corrective actions with high S scores are associated to N_4 and N_5. Corrective actions with high D scores are associated with N_6. N_3 contains corrective actions with high S and D scores. N_2 contains corrective actions with low S, O and D scores, and can be ignored.

The relationships among the six neurons can also be summarized in Fig. 4, by observing the colors code. From Fig. 4, corrective actions in N_4 and N_5 are nearest to each other (represented by yellow color), with the highest similarity measure. This can also be observed from Table 1, their weight vectors. Corrective actions in N_1 and N_4 are far to each other, with the lowest similarity measure (represented by black color). Again, this can also be observed from Table 1, their weight vectors. In this example, N_3, N_5 and N_6 have the highest RPN Intervals. The traditional RPN approach does not tell if the corrective actions are similar among each other. With Fig. 4, it can be observed that N_5 and N_6 are relatively far from each other. Corrective actions in N_5 are associated with high S scores, but, corrective actions in N_6 are associated with high D scores. In addition, it can be observed that N_3 and N_6 are relatively near to each other. Again, from Table 1, corrective actions in both N_3 and N_6 are associated of high D scores. However, corrective actions in N_3 has high S scores, and corrective actions in N_6 has medium S scores. Such approach provides additional useful information for decision makings.

4.2.3. Computation time

In this paper, a laptop equipped with Intel (R) Core (TM) i7-3612QM @3.10 GHz and 4.0 GB of RAM was used for the experimental study. The computational times required for a number of x and y settings are summarized in Table 2. From Table 2, with

Please cite this article as: W.L. Chang et al., Application of self-organizing map to failure modes and effects analysis methodology, Neurocomputing (2017), http://dx.doi.org/10.1016/j.neucom.2016.04.073

Table 2
Computation time with different x and y settings.

x	y	Computational time (in seconds)
2	2	15.351
2	3	15.326
2	4	15.431
3	3	15.347
3	4	15.720
4	4	15.743
4	5	16.164
5	5	17.177

settings $x = 2$ and $y = 3$, 15.326 s is required. With the smallest map experimented (i.e., $x = 2$ and $y = 2$), 15.351 s is required. With the largest map experimented (i.e., $x = 5$ and $y = 5$), 17.177 s is required. In short, the proposed approach could generate its topological map with a low computational requirement. Besides, the computation time increases, while the number of neuron increases.

4.3. Remarks

This empirical study demonstrates that corrective actions in FMEA can be easily visualized with SOM, which leads to the following advantages. Firstly, the corrective actions captured in a complex FMEA worksheet can be represented in a SOM map, whereby corrective actions within the same neuron share a higher similarity measure than those from other neurons. Such approach results in more effective and efficient prioritization actions and decision making. Secondly, aided by the information and knowledge elucidated from the SOM map, understanding the entire FMEA worksheet with a large number of corrective actions can be made feasible within a short period of time. Worth mentioning, research has indicated that, due to the restriction on human's span of immediate memory, only limited number of options (i.e., ≈ 7) can be effectively examined at a time [25]. With the same example, it is difficult for human to examine 77 corrective actions at a time. Organizing the 77 corrective actions to about seven, plus or minus two, groups (i.e., six groups in Section 4.2) could ease FMEA users to examine corrective actions in a more effective way. These advantages directly mitigate the challenging issues related to practical implementation of FMEA, i.e., the complexity of FMEA worksheet and its intricacy of use, as highlighted in [13,14].

5. Concluding remarks

Two important shortcomings for FMEA are the complexity of the FMEA worksheet and its intricacy of use. In this paper, a neural network clustering and visualization technique, i.e., SOM, is adopted to overcome the above-mentioned shortcomings. SOM allows corrective actions of FMEA to be clustered and visualized. Color information from SOM map is included to the FMEA worksheet for a better visualization. Besides, an RPN Interval was proposed to allow corrective actions to be ordered in groups. Experiments are conducted with benchmark information from [1] and positive results were obtained.

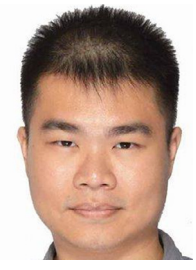
In future, the use of other clustering and visualization tools in FMEA will be investigated. More experiments will be conducted with real world information.

Acknowledgments

The financial support of the FRGS grant (i.e., FRGS/ICT02(01)/997/2013(38)) and the RACE grant (RACE/F2/TK/UNIMAS/5), are gratefully acknowledged.

References

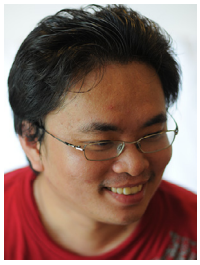
[1] D.H. Stamatis, Failure Mode and Effect Analysis: FMEA from Theory to Execution, second ed, ASQ Press, 2003.
[2] J.B. Bowles, C.E. Peláez, Fuzzy logic prioritization of failures in a system failure mode, effects and criticality analysis, Reliab. Eng. Syst. Saf. 50 (1995) 203–213.
[3] A.C.F. Guimarães, C.M.F. Lapa, Fuzzy FMEA applied to PWR chemical and volume control system, Prog. Nucl. Energy 44 (2004) 191–213.
[4] E.P. Zafiropoulos, E.N. Dialynas, Reliability prediction and failure mode effects and criticality analysis (FMECA) of electronic devices using fuzzy logic, Int. J. Qual. Reliab. Manage. 22 (2005) 183–200.
[5] K.M. Tay, C.P. Lim, Fuzzy FMEA with a guided rules reduction system for prioritization of failures, Int. J. Qual. Reliab. Manage. 23 (2006) 1047–1066.
[6] T.L. Jee, K.M. Tay, C.P. Lim, A new two-stage fuzzy inference system-based approach to prioritize failures in failure mode and effect analysis, IEEE Trans. Reliab. 64 (2015) 869–877.
[7] B.J. Garrick, The approach to risk analysis in three industries: nuclear power, space systems, and chemical process, Reliab. Eng. Syst. Saf. 23 (1988) 195–205.
[8] M.H. Korayem, A. Iravani, Improvement of 3P and 6R mechanical robots reliability and quality applying FMEA and QFD approaches, Rob. Comput. Integr. Manuf. 24 (2008) 472–487.
[9] K.M. McNally, M.A. Page, V.B. Sunderland, Failure-mode and effects analysis in improving a drug distribution system, Am. J. Health-Syst. Pharm. 54 (1997) 171–177.
[10] C.H. Jong, K.M. Tay, C.P. Lim, Application of the fuzzy failure mode and effect analysis methodology to edible bird nest processing, Comput. Electron. Agric. 96 (2013) 90–108.
[11] H.C. Liu, L. Liu, N. Liu, Risk evaluation approaches in failure mode and effects analysis: A literature review, Expert Syst. Appl. 40 (2013) 828–838.
[12] Y.W. Kerk, K.M. Tay, C.P. Lim, An analytical interval fuzzy inference system for risk evaluation and prioritization in failure mode and effect analysis, IEEE Syst. J. (2015), doi:10.1109/JSYST.2015.2478150.
[13] M.C. Signor, The failure-analysis matrix: A Kinder, gentler alternative to FMEA for information systems, in: Proceeding of Reliability and Maintainability Symposium, 2002, pp. 173–177.
[14] T.A. Montgomery, D.R. Pugh, S.T. Leedham, S.R. Twitchett, FMEA automation for the complete design process, in: Proceedings Annual Reliability & Maintainability Symposium, 1996, pp. 30–36.
[15] J.M. Legg, Computerized approach for matrix-form FMEA, IEEE Trans. Reliab. 27 (4) (1978) 254–257.
[16] J.E. Hunt, C.J. Price, M.H. Lee, Automating the FMEA process, Intell. Syst. Eng. 2 (2) (1993) 119–132.
[17] G.A. Keskin, C. Özkan, An alternative evaluation of FMEA: fuzzy art algorithm, Qual. Reliab. Eng. Int. 25 (2009) 647–661.
[18] K.M. Tay, C.H. Jong, C.P. Lim, A clustering-based failure mode and effect analysis with an application to the edible bird nest industry, Neural Comput. Appl. 26 (3) (2015) 551–560.
[19] W.L. Chang, K.M. Tay, C.P. Lim, Clustering and visualization of failure modes using an evolving tree, Expert Syst. Appl. 42 (2015) 7235–7244.
[20] G.A. Carpenter, S. Grossberg, D.B. Rosen, Fuzzy ART: fast stable learning and categorization of analog patterns by an adaptive resonance system, Neural Netw. 4 (1991) 759–771.
[21] J. Pakkanen, J. Iivarinen, E. Oja, The evolving tree – analysis and applications, IEEE Trans. Neural Netw. 17 (3) (2006) 591–603.
[22] T. Kohonen, O. Simula, A. Visa, Engineering applications of the self-organizing map, Proc. IEEE 84 (10) (1996) 1358–1384.
[23] T. Kohonen, Self-Organizing Maps, third ed., Springer, Berlin, 2001.
[24] J. Vesanto, E. Alhoniemi, Clustering of the self-organizing map, IEEE Trans. Neural Netw. 11 (3) (2000) 586–600.
[25] G.A. Miller, The magical number seven, plus or minus two: some limits on our capacity for processing information, Psychol. Rev. 63 (2) (1956) 343–352.



Wui Lee Chang received his Bachelor of Engineering in Electronic and Computer Engineering from Universiti Malaysia Sarawak, Malaysia in 2011. He is currently an MSc student at Universiti Malaysia Sarawak. His research interests include artificial neural networks and evolutionary computations, as well as failure analysis.



Lie Meng Pang received her Bachelor of Engineering in Electronic and Telecommunication Engineering from Universiti Malaysia Sarawak, Malaysia in 2012. She is currently a PhD student at Universiti Malaysia Sarawak. Her research interests include fuzzy systems and evolutionary computations.



Kai Meng Tay received his Bachelor of Engineering in Electrical and Electronic Engineering from University of Hertfordshire, UK in 2002, both MSc in Electrical and Electronic Engineering and Ph.D. degrees from Universiti Sains Malaysia, Malaysia in 2006, and 2011, respectively. He is currently a senior lecturer at Universiti Malaysia Sarawak. His research interests include fuzzy systems, and evolutionary computations, as well as failure analysis.

Please cite this article as: W.L. Chang et al., Application of self-organizing map to failure modes and effects analysis methodology, Neurocomputing (2017), http://dx.doi.org/10.1016/j.neucom.2016.04.073